Lasers in Manufacturing Conference 2015

Robust “false friend” detection via thermographic imaging

Karin Heller[a]*, Steffen Kessler[a], Friedhelm Dorsch[a], Peter Berger[b], Thomas Graf[b]

[a]*TRUMPF Laser- und Systemtechnik GmbH, Johann-Maus-Straße 2, 71254 Ditzingen, Germany*
[b]*IFSW Institut fuer Strahlwerkzeuge, Pfaffenwaldring 43, 70569 Stuttgart, Germany*

Abstract

During the laser deep penetration welding process several weld faults may occur in the solidified material and exert influence on the thermal state. The online detection of an insufficient bonding during overlap welding (commonly referred to as “false friend”) is a specific challenge, because the welding result at the upper and lower seam seems to be satisfactory, but there is no fusion between the two parts.

The experimental sensor setup provides a coaxial thermographic image of the process, which allows conclusions about changes inside the material, if they disturb the surface temperature sufficiently enough. This is the case, when a false friend prevents the heat flow to the lower part of the workpiece and a defined attribute of the thermal image is changed.

To obtain a better scientific understanding of the experimental thermographic results, the behavior of the thermal attribute is fundamentally analyzed within the scope of a simple laser welding model for which the temperature field can be computed analytically. To this case the model of Rosenthal, 1946 (reprocessed by Rykalin, 1957 and Carslaw and Jaeger, 1986) with a moving point source on the surface is adapted to a plate with finite thickness. The thermal information flow from the inside to the top surface is influenced by the processing parameters, laser power and feed rate, by the plate thickness and the material properties. The characteristics in the bulk of the material affects the top surface temperature. This becomes visible in the thermal image. Where and how this influence is detectable is investigated by taking the reflections on the bottom side of the workpiece into account.

A robust detection of a loss of fusion during an overlap welding is predicted by the analytical approach and validated by experiments.

Keywords: Welding; Process Monitoring; Thermal Imaging; Analytical Welding Models

* Corresponding author. Tel.: +49-7156-303-32908; fax: +49-7156-303-932908.
E-mail address: Karin.Heller@de.TRUMPF.com.

1. Introduction

Laser deep penetration welding is an established joining process with high energy density and fast welding speed. A series of possible welding faults is known which reduce the process quality and must be avoided. In industrial applications the insufficient bonding of two workpieces during overlap welding is a known problem. In the following, this fault is called “false friend” (FF), as in spite of the missing fusion the top and bottom surfaces of the seam suggest a good welding quality. A non-destructive examination during the welding process is possible by online thermographic imaging. The heated top surface of the workpiece emits thermal radiation, which is detected spatially resolved by a near-infrared camera and which includes information about the interior of the joint workpieces.

A loss of fusion changes the geometry and therefore the heat flow in the material. For thermographic monitoring it is necessary to have a robust indicator on the workpiece surface for a FF welding [Pfitzner et al., 2008]. Furthermore, because of a given field of view of the sensor, it is important to know the region where this indicator chances strongly enough to be detectable. Therefore, simplified analytical temperature descriptions of Rykalin, 1957 are used. The heat reflection on the insulated lower surface of the workpiece can be taken into account by integrating appropriate boundary conditions into the model. The analytical model gives a prediction for the attribute change during the occurrence of a FF in a specified welding process, which can be compared with experimental results.

The simplified model to estimate how strong and where the identified attribute changes under a loss of fusion, it is predicted under which circumstances the FF welding can be detected by thermographic imaging .

2. False friend (FF) occurrence: Process and sensor setup

The scope of this article is deep penetration laser welding of an overlap configuration of two zinc-coated steel plates. Due to the low evaporation temperature of zinc, a gap between the two welding parts is necessary to provide space for the zinc vapor. This gap has to be small enough that the molten material can bridge this gap and connect the components. If the gap is too large, there is no fusion in the inside of the welding seam, leading to a “false-friend welding”, see Fig. 1).

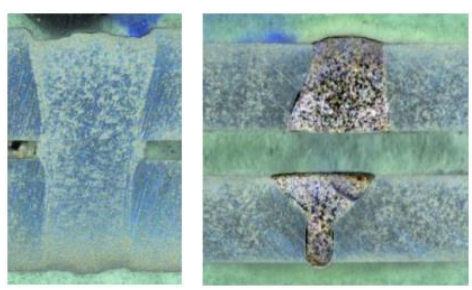

Fig. 1. Cross section of an overlap weld with fusion (*left*) and missing fusion (*right*), in case of a sheet configuration exceeding the permissible gap height.

The change of heat flow and top surface temperature, which occur for a FF, motivates a thermographic monitoring of the process. To realize such a monitoring, an InGaAs camera is coaxially integrated in different TRUMPF welding optics, such as the BEO-D70 or the scanner optics PFO 3D. The experimental setup is illustrated in Fig. 2.

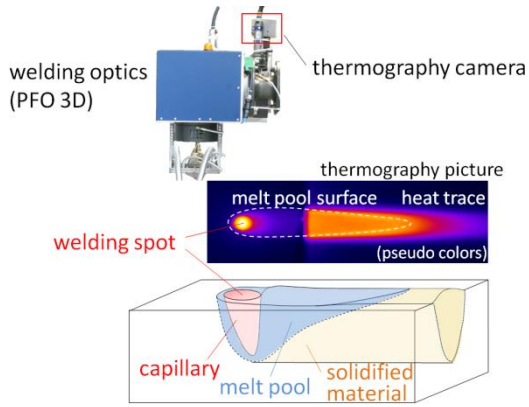

Fig. 2. Sensor setup with a thermography camera attached to a PFO 3D scanner optics. Additionally, an example of a thermography image of the workpiece surface is shown.

3. Analytical model

The simplified model expands the stationary model of a point source on a plate with infinite thickness [Rykalin, 1957] to the case of a plate with finite thickness. A point source uniformly moves on the surface and heats the workpiece until a steady state of the temperature field around the source is reached. The frame of reference (FOR) for the temperature distribution is always co-moving with the heat source. The material properties are assumed to be constant and phase transitions are neglected. By using the method of image sources, the heat reflection on the insulated workpiece boundaries can be taken into consideration. The point source with the external sources is shown in Fig. 3. The arrows represent the heat flow as determined by the reflection at the top and bottom workpiece surface. The steady state temperature distribution of the model, given in Rykalin, 1957, uses a semi-infinite body, i.e. a temperature field in a plate with infinite thickness. Here, a finite plate thickness is integrated by assuming insulated surfaces at the top and bottom of the workpiece. The heat reflections at the insulated surfaces can be taken into account by using image sources, whose positions can be obtained by alternately reflecting the source at the bottom and top surface (see Fig. 3). The resulting temperature field arises out of the contributions of all heat sources. For a given point in the workpiece the contributions of succeeding image sources becomes steadily smaller so that (most often) a finite number of image sources gives a good approximation of the temperature value at that point.

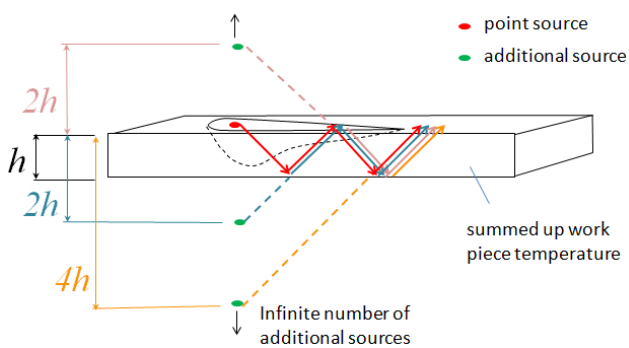

Fig. 3. Workpiece with finite thickness (heat reflection on the bottom side) and temperature influencing point sources of the simplified analytical welding model.

During overlap weldings the upper sheet is, in general, more heated than the lower sheet. Compared with experiments the model of the point source on the top surface leads to a good representation of the real temperature field of the welding process.

Within the scope of this model the cases of fusion and no fusion are modeled by the following assumptions: In case of no fusion there is no heat transfer between the upper and the lower plate, as the lower plate is irrelevant. This corresponds to the case of a single sheet with the thickness of the upper plate. In case of fusion the heat flows from the upper to the lower plate through the seam and the model is simplified to a single plate whose thickness is the sum of the thickness of the upper and the lower plate. By allowing the heat to flow to the lower sheet through the whole interface, the heat flow is slightly overestimated.

4. Temperature on the top surface influenced by a "false friend" (FF)

The information from changed heat flow distributions due to a changed geometry in the inside of the workpiece becomes visible on the top surface at a distance d behind the source. To get an idea, where the temperature change due to inner processes can be detected on the top surface, the track of the heat reflection of a point source is shown in Fig. 4.

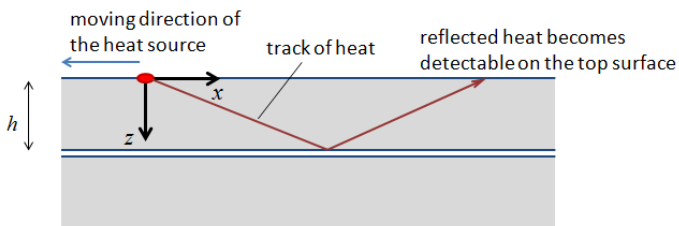

Fig. 4. Track of the heat of a point source in a plate with finite thickness.

To analyze the temperature distribution behind the moving heat source, the two kinds of heat transport are taken into account: the heat transport due to heat conduction, where the covered distance $|\boldsymbol{x}|$ is proportional to the square root of the product of the thermal diffusivity α and the time t

$$|\boldsymbol{x}| \sim \sqrt{\alpha t}\,, \qquad (1)$$

and the heat transport due to the co-moving FOR, where the distance $|\boldsymbol{x}|$ is equal to the product of the feed rate v and the time t

$$|\boldsymbol{x}| \sim vt\,. \qquad (2)$$

The different transport mechanisms of the heat are dominant in the different directions. Under typical welding conditions ($h \gg \alpha/v$), the horizontal heat transport in x-direction is dominated by the ballistic heat transport described by equation (2). The vertical heat transport in z-direction only consists of the heat conduction process according equation (1). For the vertical heat flow, to the bottom and back to the top, the time $t \sim z^2/\alpha$ is needed with $z = 2h$. During this time, the advection leads to a (horizontal) movement with distance

$$d \sim h^2\, v/\alpha\,. \qquad (3)$$

This result shows the scaling behavior of the distance to the source at which the influence of the plate thickness becomes strong enough to be detectable. This distance scales with the square of the plate thickness and is proportional to the feed rate.

It is expected that in case of a loss of fusion the temperature will hardly change in a region smaller than this distance and that there is a significant change in the region beyond this distance.

5. Experimental and analytical determination of false friend

In this section an attribute sensitive to a FF is defined which can be measured experimentally by thermographic imaging and whose change due to a loss of fusion can be estimated by the analytical model. The thermal image (see left part of Fig. 5) represents the radiant emittance I_R from the heated workpiece surface. A plot and a logarithmic plot of a profile section along the center line of the seam are shown in the right part of Fig. 5.

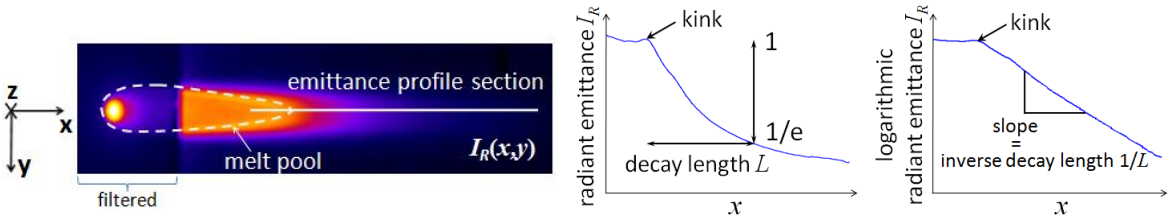

Fig. 5. Thermal image with filtered area for key hole observations, and the profile section of the radiant emittance I_R across the x-axis (direct intensity value and logarithmized).

The end of the melt pool is given by a kink in the profile, due to the melting enthalpy and a kink in the emissivity at the phase transformation [Pfitzner et al., 2008]. Typically, the decay of radiation from the solidified heat trace is close to an exponential decay, which becomes evident in the logarithmic plot [Pfitzner et al., 2008]. Hence, as characterizing value the exponential "length constant" called decay length L is well suited as a quantifiable attribute of the cooling process along the welding direction [Dorsch et al., 2013]. To obtain the decay length out of the thermal image a straight line is fitted to the logarithmic profile section and the slope determines the decay length L.

The upper sheet is in general more heated than the lower sheet. In case of fusion there is a strong heat flow from the upper to the lower sheet. This heat flow vanishes when the fusion is lost (FF). Therefore, the cooling of the upper part is reduced and an increase of the decay length is expected.

Within the scope of the described model of section 3 the temperature along the line behind the source $T_L(x)$ can be computed analytically if the source power, feed rate, plate thickness and the thermal diffusivity of the material are known. From the detected radiant emittance, conclusions to the temperature distribution are possible. This is compared with the analytical profile by assuming Wien's law with a constant emissivity

$$\ln I_R(x) \sim -\frac{T_R}{T_L(x)}\,, \tag{4}$$

where $T_R = c_R/\lambda_0$ is called observation temperature (depending on the observation wavelength λ_0) with $c_R = h_P c_0/k_B \approx 0.0144\ \mathrm{Km}$. For a wavelength within the spectral range of $\lambda_0 = 1.5 \ldots 1.6\ \mu\mathrm{m}$ the observation temperature $T_R = 9\,000 \ldots 10\,000\ \mathrm{K}$ is much higher than the temperature of the solid phase for steel ($T < 1800\ \mathrm{K}$), justifying the use of Wien's approximation. Using this connection together with the definition of the decay length, the (local) decay length can be computed by the gradient of the temperature along the seam direction

$$L(x) = \left(\frac{\partial}{\partial x}\frac{T_R}{T_L(x)}\right)^{-1} \tag{5}$$

depending on the location.

6. Experimental validation

While the experimental decay length in section 5 is determined by the averaged slope of the logarithmized radiant emittance I_R (see diagram on the right in Fig. 5), the analytically determined value depends on the location (see equation 5), but it can be averaged over a local range to gain a comparable value.

The definition of the decay length is motivated by its increase in case of a loss of fusion. For an analytical estimation of the influence of a FF, the model of a point source in the upper plate of finite thickness is used, where the two plates have the same thickness. The analytically obtained temperature of the correct fusion is computed under same conditions but with double of the plate thickness (see section 3).

To show the change in the decay length when fusion is lost and to compare the results to experiments, the process parameters ($P = 2{,}5$ kW, $v = 4$ m/min) are used exemplarily. The thickness of the two plates of mild steel is 1 mm each.

The case of a plate thickness of 1 mm (no fusion - FF) and 2 mm (total fusion) are compared. The analytical model leads to decay lengths which are depicted in the left picture of Fig. 6 together with their ratio in the right picture. As explained in section 4, the effect of a change in the plate thickness changes the temperature field significantly after a certain distance behind the source. Close to the source the decay lengths are approximately identical (see Fig. 6, left). For larger distances the curves separate with a higher decay length in case of no fusion. Correspondingly, the ratio is close to 1 for short distances and increases to a maximum value of about 2.5 at about 8 mm, before decreasing asymptotically to the ratio of the plate thicknesses (here 2) in the far field (see Fig. 6, right). In the experiments the decay lengths are averaged over a region up to about 5 mm behind the melt pool end. The analytical prediction in that region is consistent with the experimentally measured values. This example shows that the decay length is a strong indicator for a false friend. In the heat trace close to the melt pool, where the sensor detects the thermal radiation, the decay length is more than doubled (≈ 2.4, see Fig. 6, right) compared to the case of a correct fusion. In cases of thicker plates or a higher feed rate the region where the decay length changes significantly starts at larger distance to the source.

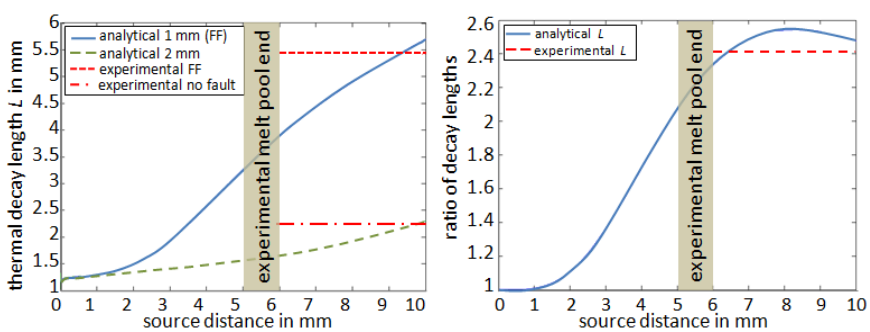

Fig. 6. *Left:* Decay length progression for a point source in a finite plate with 1 mm and 2 mm, *Right:* The ratio of the decay length shown in the left picture. The (red) horizontal lines indicate the experimental determined values. (BEO D70 optics, welding parameters: power 2.5 kW, feed rate 4 m/min, material S235, focus -2 mm).

In Fig. 7 the ratio of the decay lengths for both cases (FF and correct fusion) is shown for different welding parameters. The analytical mean values and the experimental ratios match quiet well, except of the welding with $P = 3\ \mathrm{kW}$ and $v = 4\ \mathrm{m/min}$. It is assumed, that the deviation follows from the high dynamics of the laser welding process, which can lead to wide fluctuations in the experimentally obtained radiation images.

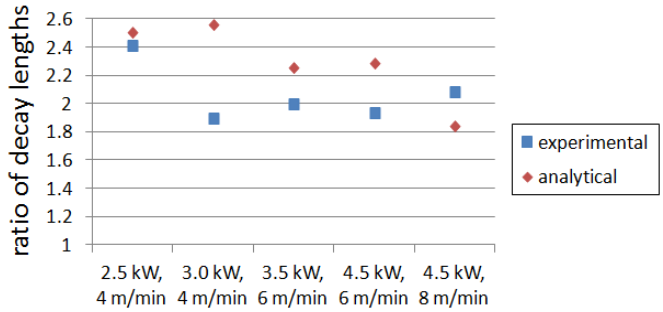

Fig. 7. Experimentally and analytically obtained values for the ratio of the decay length for the cases of a FF and a fusion for different values of power and feed rate (remaining process parameters as in Fig. 6).

Obviously, the decay length is a good indicator to identify a FF, which changes by a factor of about 2 in the presented examples.

7. Summary and Conclusion

It is shown that online thermographic imaging is able to detect a loss of fusion in overlap weld joints. With a simplified model the influence of the change of plate thickness on the surface temperature is analyzed. It is shown that close to the source the change is too small to be detected by measurements. Starting at a certain distance, the change is strong enough to be detected. Within the scope of the model this distance scales with the square of the plate thickness and linear with the feed rate of the source. Hence, for the thermographic imaging the viewing field behind the source has to be sufficiently long (depending on plate thickness and feed rate) to be able to detect geometric changes at the lower plate.

The decay length characterizes the cooling along the seam. It is identified as a strong indicator for a loss of fusion in overlap welding. It can be obtained experimentally by an online thermographic process monitoring. The increase in the decay length in case of a loss of fusion corresponds to a limited cooling of the upper plate and can be estimated within the limits of a simple model. Experiments show qualitative and to some extend quantitative agreement between the analytical results and the measurements.

References

Rosenthal, D., 1946. The Theory of Moving Sources of Heat and its Application to Metal Treatments, In: Transcription of the ASME 68; s. 849-866

Rykalin, N., 1957. Berechnung der Wärmevorgänge beim Schweißen, Berlin: VEB-Verlag

Carslaw, H. S., Jaeger, J. C., 1986. Conduction of heat in solids, Oxford Oxfordshire New York: Carendon Press Oxford University Press, ISBN 0198533683

Pfitzner, D., Hesse, T., Magg, W., 2008. Verfahren zum Erkennen von Fehlern an einer Schweißnaht während eines Laser-Schweißprozesses, Patent Trumpf Werkzeugmaschinen GmbH + Co. KG DE 10 2007 024 789 A1 2008.10.23

Dorsch, F., et al., 2013. High-productivity welding processes using brilliant laser beam sources through quantitative process diagnostics and control / MABRILAS Concept: Joint project WELDone. (FKZ:13N10681) final report